THE EUROPEAN
PHYSICAL JOURNAL C

Dilaton-induced open quantum dynamics

Christian Käding[a] , **Mario Pitschmann**[b] , **Caroline Voith**[c]

Technische Universität Wien, Atominstitut, Stadionallee 2, 1020 Vienna, Austria

Abstract In modern cosmology, scalar fields with screening mechanisms are often used as explanations for phenomena like dark energy or dark matter. Amongst a zoo of models, the environment dependent dilaton, screened by the Polyakov–Damour mechanism, is one of the least constrained ones. Using recently developed path integral tools for directly computing reduced density matrices, we study the open quantum dynamics of a probe, modelled by another real scalar field, induced by interactions with an environment comprising fluctuations of a dilaton. As the leading effect, we extract a correction to the probe's unitary evolution, which can be observed as a frequency shift. Assuming the scalar probe to roughly approximate a cold atom in matter wave interferometry, we show that comparing the predicted frequency shifts in two experimentally distinct setups has the potential to exclude large parts of the dilaton parameter space.

1 Introduction

In modern cosmology, scalar-tensor theories of gravity [1], in which scalar fields are coupled to the gravitational metric tensor, are often proposed as potential solutions for the problems of dark matter and dark energy, see Refs. [2,3] for an overview. In many cases, such scalar-tensor theories lead to a universal coupling of the scalar to the trace T^{μ}_{μ} of the matter energy-momentum tensor. Consequently, these theories predict the existence of gravity-like fifth forces. However, to date, we did not observe any additional fundamental forces beyond the four known ones, which is reflected in strong Solar System constraints [4–6].

A phenomenologically interesting way of explaining the apparent absence of fifth forces in our Solar System is via a so-called screening mechanism. Such mechanisms can arise in non-linear scalar field theories, and induce a screening of the scalar's fifth force, i.e. render it to be very weak, in environments with large values of T^{μ}_{μ}, for example, for high densities $\rho^{\text{ext}} = -T^{\mu}_{\mu}$ in dust-dominated regions like our Solar System. By now, there are several scalar models which exhibit a screening mechanism [7,8]. Amongst the most prominent so-called screened scalar fields are: the chameleon [9,10]; the symmetron [11–18], whose fifth force has recently been studied as an alternative to particle dark matter [19–22]; the environment dependent dilaton [13,23–28]; and the galileon [29–31]. Many of these models have already been or are proposed to be tested in a plethora of experiments, see, for example, Refs. [7,32–48]. In addition, in recent years, research programs were initiated to study screened scalars as quantum fields [49–52], and it was even suggested to investigate screened scalar-tensor theories in analogue gravity simulations [53].

Reference [50] presented the idea for using open quantum dynamical effects [54] like frequency shifts or decoherence [55], which might be induced by interactions with an environment comprising light scalar fluctuations, for further constraining chameleon screened scalar fields in atom interferometry experiments. Besides presenting phenomenological research, Ref. [50] also introduced a novel and powerful theoretical tool, namely a practicable and first principle-based method for deriving quantum master equations for reduced density matrices in scalar quantum field theory. This method relies on the Schwinger–Keldysh formalism [56,57] and the Feynman–Vernon influence functional [58]. Based on the work in Ref. [50], Ref. [59] developed a way of circumventing master equations by directly computing reduced density matrix elements with influence functionals. In addition, Ref. [60] derived a similar technique for computing total density matrices in interacting quantum field theories.

In this article, we look at the environment dependent dilaton screened scalar field as a yet barely constrained model.

a e-mail: christian.kaeding@tuwien.ac.at (corresponding author)

b e-mail: mario.pitschmann@tuwien.ac.at

c e-mail: e1607478@student.tuwien.ac.at

Following the approach made in Ref. [50], we study the open quantum dynamics of a probe real scalar field ϕ when interacting with an environment comprising fluctuations χ of a dilaton field X. More precisely, we use the scalar ϕ as a proxy for an atom in an atom interferometry experiment (or any other object in a matter interferometer, e.g., neutrons) and, applying the formalism from Ref. [59], check how its reduced density matrix evolves from an initial time 0 to a final time t due to the hypothetical interaction with a dilaton. We then read off the most dominant open quantum dynamical effect induced in the probe system ϕ in order to get an estimate of the dilaton parameter space that could be constrained experimentally this way.

Certainly, using a scalar field ϕ as a proxy for a more complex object like an atom has its shortcomings. However, since the dilaton only couples to the trace of the atom's energy-momentum tensor, a scalar field is a rough but, in this case, suitable first approximation. In order to improve this approximation, we consider the probe system being restricted to a single-particle subspace and ignore all ϕ-loop diagrams, which naturally appear in a scalar quantum field theory, but are unrealistic for a complex and stable object like a cold atom.

Providing a glance at the full potential that open quantum dynamical effects can have for constraining physics beyond the standard models of particles and cosmology, this article presents a first application of Ref. [59], and motivates future studies with more realistic and sophisticated probe models.

The article is structured as follows: at first, we review the environment dependent dilaton model in Sect. 2. Subsequently, we take the required formula from Ref. [59], discuss and evaluate it in Sect. 3, and then use the results for estimating constraints for the dilaton parameter space in Sect. 4. Finally, in Sect. 5, we draw our conclusions.

2 Environment dependent dilatons

Dilatons originate from string theory [13,24,25], but have found applications in cosmology [23,27] and were shown, similar to symmetrons, to be subject to the Polyakov–Damour mechanism [13], which coins them to be environment dependent [26] and therefore a screened scalar field model.

The environment dependent dilaton has an effective potential [3]

$$V_{\text{eff}}(\varphi; \rho^{\text{ext}}) = \bar{V}_0 \, e^{-\varphi/M_{Pl}} + \frac{(\varphi - \varphi_*)^2}{2\mathcal{M}^2} \rho^{\text{ext}}, \tag{1}$$

where $\bar{V}_0$ is a constant potential with a decreasing exponential function $\exp(-\varphi/M_{Pl})$ as required by the strong coupling limit of string theory. Here, M_{Pl} denotes the Planck mass, $\mathcal{M}$ is a coupling constant with dimension of a mass, for which we require $\varphi \ll \mathcal{M}$, and φ_* is a constant field value around

which the coupling of the dilaton to matter becomes feeble or even vanishes entirely for $\varphi = \varphi_*$. This decoupling is the essence of the Polyakov–Damour mechanism and leads to a suppression of the dilaton fifth force.

The fact that a larger value of ρ^{ext} actually corresponds to a weaker coupling to matter can more easily be seen when substituting $\lambda X := \varphi - \varphi_*$ into Eq. (1). Introducing

$$V(X) := V_0 \, e^{-\lambda X/M_{Pl}} := \bar{V}_0 \, e^{-(\lambda X + \varphi_*)/M_{Pl}} \tag{2}$$

with λ being a dimensionless coupling constant, we find [28]

$$V_{\text{eff}}(X; \rho^{\text{ext}}) = V_0 \, e^{-\lambda X/M_{Pl}} + \frac{A_2 \rho^{\text{ext}}}{2M_{Pl}^2} X^2, \tag{3}$$

where a dimensionless constant $A_2 := \lambda^2 M_{Pl}^2/\mathcal{M}^2$ was introduced that has to fulfill $A_2 \gg 1$ in order to circumvent existing Solar System-based constraints on scalar fifth forces [16]. From Eq. (3) we find the dilaton vacuum expectation value (vev) as [28]

$$\langle X \rangle = \frac{M_{Pl}}{\lambda} W \left(\frac{\lambda^2 V_0}{A_2 \rho^{\text{ext}}} \right) \tag{4}$$

with the Lambert W-function

$$W(x) = \sum_{n=1}^{\infty} \frac{(-n)^{n-1}}{n!} x^n. \tag{5}$$

Since $X = \langle X \rangle + \chi$, where χ is a small perturbation, Eq. (4) lets us conclude that X decreases when ρ^{ext} increases. Consequently, the leading $\langle X \rangle^2$-term in Eq. (3) becomes smaller for larger values of ρ^{ext}, which indicates a decoupling between dilaton and matter, i.e. a screening of the fifth force.

As a scalar-tensor theory, the dilaton is coupled to the gravitational metric tensor via $\tilde{g}_{\mu\nu} = A^2(X)g_{\mu\nu}$, where $\tilde{g}$ and g denote the metric in the Jordan and Einstein frame [1], respectively, and the conformal factor is given by

$$A(X) = 1 + \frac{A_2}{2M_{Pl}^2} X^2. \tag{6}$$

The total Einstein frame action describing gravity, the scalar X and matter is given by [9,10]

$$S = \int d^4x \sqrt{-g} \left[\frac{1}{2} M_{Pl}^2 R - \frac{1}{2} g^{\mu\nu} \partial_\mu X \partial_\nu X - V(X) \right] + \int d^4x \sqrt{-g} A^4(X) \tilde{\mathcal{L}}_M(\tilde{\phi}, A^2(X)g_{\mu\nu}), \tag{7}$$

where the last term describes the dynamics of the Jordan frame matter field $\tilde{\phi}$, which in our case is a real scalar, and its interactions with the dilaton. Here, the potential $V(X)$ is the self-interaction of X given by Eq. (2), and for the Jordan frame matter Lagrangian we use

$$\tilde{\mathcal{L}}_M = -\frac{1}{2} \tilde{g}^{\mu\nu} \partial_\mu \tilde{\phi} \partial_\nu \tilde{\phi} - \frac{1}{2} \tilde{M}^2 \tilde{\phi}^2. \tag{8}$$

Since we will have to work with the dilaton perturbatively if we later want to discuss it in the formalism presented in Ref. [59], we are required to assume $\lambda X / M_{Pl} \ll 1$, such that we can expand

$$V(X) \approx V_0 \left[1 - \frac{\lambda}{M_{Pl}} X + \frac{1}{2} \frac{\lambda^2}{M_{Pl}^2} X^2 + \mathcal{O}\left(\frac{\lambda^3}{M_{Pl}^3} X^3 \right) \right].$$
(9)

Following the general procedure outlined in Ref. [50] for Eqs. (6)–(9), while only keeping operators of dimension 4 or lower, we can derive Einstein frame free actions for the matter field ϕ and the dilaton fluctuation χ as well as an interaction action between both types of fields:

$$S_\phi[\phi] := \int_x \left[-\frac{1}{2} g^{\mu\nu} \partial_\mu \phi \partial_\nu \phi - \frac{1}{2} M^2 \phi^2 \right],$$
(10)

$$S_\chi[\chi] := \int_x \left[-\frac{1}{2} g^{\mu\nu} \partial_\mu \chi \partial_\nu \chi - \frac{1}{2} m^2 \chi^2 \right],$$
(11)

$$S_{\text{int}}[\phi, \chi] := \int_{x \in \Omega_t} \left[-\frac{1}{2} \alpha_1 M \chi \phi^2 - \frac{1}{4} \alpha_2 \chi^2 \phi^2 \right],$$
(12)

where, using $g_{\mu\nu} \equiv \eta_{\mu\nu}$ from now on,

$$\int_x := \int d^4 x,$$
(13)

the masses are

$$M^2 := \left(1 + \frac{A_2}{M_{Pl}^2} \langle X \rangle^2 \right) \tilde{M}^2$$

$$m^2 \approx \frac{1}{M_{Pl}^2} \left(V_0 \lambda^2 + A_2 \rho^{\text{ext}} \right),$$
(14)

the coupling constants take on the forms

$$\alpha_1 := 2M \frac{A_2}{M_{Pl}^2} \langle X \rangle \left(1 - \frac{A_2}{M_{Pl}^2} \langle X \rangle^2 \right), \quad \alpha_2 := \frac{M}{\langle X \rangle} \alpha_1,$$
(15)

and we restrict integrations over spacetime coordinates to $\Omega_t := [0, t] \times \mathbb{R}$ since we are only interested in the finite interval between initial time 0 and final time t. Note that at the order considered in the expansion made in Eq. (9) the dilaton does not self-interact and, therefore, we do not need to consider a self-interaction action for χ.

3 Open quantum dynamics

Most realistic quantum systems should be treated as open, i.e. as interacting with one or several environments. Such interactions can induce open quantum dynamical effects like frequency (or phase) shifts or decoherence in a system. While the theory of open quantum systems naturally finds many applications in non-relativistic quantum physics,

see e.g. Refs. [61–67], it also receives increased attention in quantum field theory [50,68–76], and adjacent areas like Early Universe cosmology [77–89], black holes [90–96], or heavy-ion physics [97–106].

Quantum systems, especially open ones, are often described by density operators $\hat{\rho}(t)$, which are advantageous over a wave function description since they can not only describe pure but also mixed states. This is necessary in order to fully capture phenomena like decoherence. In case of an open quantum system, we usually work with reduced density operators, which are obtained by tracing out the environmental degrees of freedom.

Projecting a (reduced) density operator into a basis, for example, a single-particle momentum basis as we will use in this article, gives elements of a density matrix:

$$\rho(\mathbf{p}; \mathbf{p}'; t) = \langle \mathbf{p} | \hat{\rho}(t) | \mathbf{p}' \rangle.$$
(16)

The time evolution of density matrices can be described by quantum master equations. However, such equations are often analytically intricate or even impossible to solve. In order to avoid such complications, using the technology presented in Ref. [50], Ref. [59] developed a formalism that enables us to directly compute reduced density matrices in terms of the Feynman–Vernon influence functional [58], which itself is based on the Schwinger–Keldysh formalism [56,57].

In this article, we consider an open quantum system ϕ, which is a proxy for an atom (or another, compared to the dilaton relatively heavy matter particle like a neutron) with zero temperature in order to justify a restriction to the single-particle subspace. As was pointed out in Refs. [50,59], in this case, contractions of the system field can only give rise to Feynman and Dyson propagators:

$$\overrightarrow{\phi_x^+ \phi_y^+} = D_{xy}^{++} = D_{xy}^{\text{F}} = -i \int_k \frac{e^{ik \cdot (x-y)}}{k^2 + M^2 - i\epsilon},$$
(17)

$$\overrightarrow{\phi_x^- \phi_y^-} = D_{xy}^{--} = D_{xy}^{\text{D}} = +i \int_k \frac{e^{ik \cdot (x-y)}}{k^2 + M^2 + i\epsilon},$$
(18)

where

$$\int_k := \int \frac{d^4 k}{(2\pi)^4},$$
(19)

and $+$ and $-$ denote the positive and negative branches of the Schwinger–Keldysh closed time path, respectively.

The system is interacting with an environment comprised of dilaton fluctuations χ. As was also done in Ref. [50] for the chameleon, we assume the dilaton to have a, in general, non-zero temperature T, for example, due to thermalization with the walls of a vacuum chamber in an atom interferometry experiment. This means, open system and environment are out of thermal equilibrium in our discussion. Since environmental degrees of freedom can be contracted for any combination of $+$ and $-$ [50,59], the dilaton can give Feynman

and Dyson, but also Wightman propagators:

$$
\overline{\chi_x^+ \chi_y^+} = \Delta_{xy}^{++} = \Delta_{xy}^{\mathrm{F}} = -\mathrm{i} \int_k e^{\mathrm{i}k\cdot(x-y)}
$$
$$
\times \left[\frac{1}{k^2 + m^2 - \mathrm{i}\epsilon} + 2\pi \mathrm{i} f(|k^0|)\delta(k^2 + m^2) \right],
\tag{20}
$$

$$
\overline{\chi_x^- \chi_y^-} = \Delta_{xy}^{--} = \Delta_{xy}^{\mathrm{D}} = +\mathrm{i} \int_k e^{\mathrm{i}k\cdot(x-y)}
$$
$$
\times \left[\frac{1}{k^2 + m^2 + \mathrm{i}\epsilon} - 2\pi \mathrm{i} f(|k^0|)\delta(k^2 + m^2) \right],
\tag{21}
$$

$$
\overline{\chi_x^+ \chi_y^-} = \langle \chi_y \chi_x \rangle = \Delta_{xy}^{+-} = \Delta_{xy}^{<}
$$
$$
= \int_k e^{\mathrm{i}k\cdot(x-y)} 2\pi \, \mathrm{sgn}(k^0) f(k^0)\delta(k^2 + m^2),
\tag{22}
$$

$$
\overline{\chi_x^- \chi_y^+} = \langle \chi_x \chi_y \rangle = \Delta_{xy}^{-+} = \Delta_{xy}^{>}
$$
$$
= \Delta_{yx}^{<} = (\Delta^{<})_{xy}^{*},
\tag{23}
$$

where

$$
f(k^0) := \frac{1}{e^{\beta k^0} - 1} = -[1 + f(-k^0)]
\tag{24}
$$

is the Bose-Einstein distribution function with $\beta = 1/T$ being the inverse temperature.

Following Ref. [59], the reduced density matrix element for ϕ at time t in the single-particle momentum subspace, under the assumption that the system's particle number does not change in the interval $[0, t]$, can be obtained by evaluating

$$
\rho(\mathbf{p}; \mathbf{p}'; t) = \lim_{\substack{x^{0(\prime)} \to t^+ \\ y^{0(\prime)} \to 0^-}} \int_{\mathbf{k}\mathbf{k}'} \frac{\rho(\mathbf{k}; \mathbf{k}'; 0)}{(2E_{\mathbf{k}}^{\phi})(2E_{\mathbf{k}'}^{\phi})}
$$
$$
\times \int_{\mathbf{x}\mathbf{x}'\mathbf{y}\mathbf{y}'} e^{-\mathrm{i}(\mathbf{p}\cdot\mathbf{x}-\mathbf{p}'\cdot\mathbf{x}')+\mathrm{i}(\mathbf{k}\cdot\mathbf{y}-\mathbf{k}'\cdot\mathbf{y}')}
$$
$$
\times \partial_{x^0, E_{\mathbf{p}}^{\phi}} \partial_{x^{0\prime}, E_{\mathbf{p}'}^{\phi}}^{*} \partial_{y^0, E_{\mathbf{k}}^{\phi}}^{*} \partial_{y^{0\prime}, E_{\mathbf{k}'}^{\phi}}
$$
$$
\times \int \mathcal{D}\phi^{\pm} e^{\mathrm{i}\{S_\phi[\phi^+] - S_\phi[\phi^-]\}} \phi_x^+ \phi_{x'}^-
$$
$$
\times \mathcal{F}[\phi^{\pm}; t] \phi_y^+ \phi_{y'}^-,
\tag{25}
$$

where the Feynman–Vernon influence functional

$$
\mathcal{F}[\phi^{\pm}; t] = \left\langle e^{\mathrm{i}\{S_{\mathrm{int}}[\phi^+, \chi^+; t] - S_{\mathrm{int}}[\phi^-, \chi^-; t]\}} \right\rangle_\chi
\tag{26}
$$

is given in terms of the expectation value

$$
\langle A[\chi^a] \rangle_\chi := \int d\chi_t^{\pm} d\chi_0^{\pm} \delta(\chi_t^+ - \chi_t^-) \rho_\chi[\chi_0^{\pm}; 0]
$$
$$
\times \int_{\chi_0^{\pm}}^{\chi_t^{\pm}} \mathcal{D}\chi^{\pm} A[\chi^a] e^{\mathrm{i}\{S_\chi[\chi^+] - S_\chi[\chi^-]\}}
\tag{27}
$$

with $\rho_\chi[\chi_0^{\pm}; 0]$ denoting the initial environmental density matrix under the assumption that system and environment

were initially uncorrelated. The index of a field, e.g. t on χ_t, labels the time slice on which the field eigenstate was taken.

We expand the Feynman–Vernon influence functional up to second order in the coupling constants α_1 and α_2, and find

$$
\mathcal{F}[\phi^{\pm}; t] = 1 - \mathrm{i}\frac{\alpha_2}{4} \sum_{a=\pm} a \int_x (\phi_x^a)^2 \Delta_{xx}^{\mathrm{F}}
$$
$$
- \frac{1}{2} \sum_{a,b=\pm} ab \int_{xy} \left[\frac{\alpha_1^2 M^2}{4} (\phi_x^a)^2 (\phi_y^b)^2 \Delta_{xy}^{ab} \right.
$$
$$
\left. + \frac{\alpha_2^2}{16} (\phi_x^a)^2 (\phi_y^b)^2 \left(\Delta_{xx}^{\mathrm{F}}\Delta_{yy}^{\mathrm{F}} + 2(\Delta_{xy}^{ab})^2 \right) \right]
$$
$$
+ \mathcal{O}\left(\alpha_{1,2}^3\right).
\tag{28}
$$

Substituting Eq. (28) into Eq. (25), using Wick's theorem [107], and dropping every term containing ϕ-loops, we obtain

$$
\rho(\mathbf{p}; \mathbf{p}'; t) = \lim_{\substack{x^{0(\prime)} \to t^+ \\ y^{0(\prime)} \to 0^-}} \int_{\mathbf{k}\mathbf{k}'} \frac{\rho(\mathbf{k}; \mathbf{k}'; 0)}{(2E_{\mathbf{k}}^{\phi})(2E_{\mathbf{k}'}^{\phi})}
$$
$$
\times \int_{\mathbf{x}\mathbf{x}'\mathbf{y}\mathbf{y}'} e^{-\mathrm{i}(\mathbf{p}\cdot\mathbf{x}-\mathbf{p}'\cdot\mathbf{x}')+\mathrm{i}(\mathbf{k}\cdot\mathbf{y}-\mathbf{k}'\cdot\mathbf{y}')}
$$
$$
\partial_{x^0, E_{\mathbf{p}}^{\phi}} \partial_{x^{0\prime}, E_{\mathbf{p}'}^{\phi}}^{*} \partial_{y^0, E_{\mathbf{k}}^{\phi}}^{*} \partial_{y^{0\prime}, E_{\mathbf{k}'}^{\phi}}
$$
$$
\times \left\{ D_{xy}^{\mathrm{F}} D_{x'y'}^{\mathrm{D}} \right.
$$
$$
- \mathrm{i}\frac{\alpha_2}{2} \int_z \left[D_{xz}^{\mathrm{F}} D_{zy}^{\mathrm{F}} D_{x'y'}^{\mathrm{D}} - (x, y \longleftrightarrow x', y')^* \right] \Delta_{zz}^{\mathrm{F}}
$$
$$
- \frac{\alpha_1^2 M^2}{8} \int_{zz'} \left[\left(D_{x'y'}^{\mathrm{D}} \left(8 D_{xz}^{\mathrm{F}} D_{zz'}^{\mathrm{F}} D_{z'y}^{\mathrm{F}} + 2 D_{xy}^{\mathrm{F}} D_{zz'}^{\mathrm{F}} D_{zz'}^{\mathrm{F}} \right) \Delta_{zz'}^{\mathrm{F}} \right. \right.
$$
$$
+ (x, y \longleftrightarrow x', y')^* \Big)
$$
$$
- \left(8 D_{xz}^{\mathrm{F}} D_{zy}^{\mathrm{F}} D_{x'z'}^{\mathrm{D}} D_{z'y'}^{\mathrm{D}} + 4 D_{xy}^{\mathrm{F}} D_{zz}^{\mathrm{F}} D_{x'z'}^{\mathrm{D}} D_{z'y'}^{\mathrm{D}} \right) \Delta_{zz'}^{+-} \right]
$$
$$
- \frac{\alpha_2^2}{32} \int_{zz'} \left[\left(D_{x'y'}^{\mathrm{D}} \left(8 D_{xz}^{\mathrm{F}} D_{zz'}^{\mathrm{F}} D_{z'y}^{\mathrm{F}} + 2 D_{xy}^{\mathrm{F}} D_{zz'}^{\mathrm{F}} D_{zz'}^{\mathrm{F}} \right) \right. \right.
$$
$$
\left(\Delta_{zz}^{\mathrm{F}}\Delta_{z'z'}^{\mathrm{F}} + 2(\Delta_{zz'}^{\mathrm{F}})^2 \right) + (x, y \longleftrightarrow x', y')^* \Big)
$$
$$
- \left(8 D_{xz}^{\mathrm{F}} D_{zy}^{\mathrm{F}} D_{x'z'}^{\mathrm{D}} D_{z'y'}^{\mathrm{D}} \right.
$$
$$
\left. \left. + 4 D_{xy}^{\mathrm{F}} D_{zz}^{\mathrm{F}} D_{x'z'}^{\mathrm{D}} D_{z'y'}^{\mathrm{D}} \right) \left(\Delta_{zz}^{\mathrm{F}}\Delta_{z'z'}^{\mathrm{F}} + 2(\Delta_{zz'}^{+-})^2 \right) \right] \right\}.
\tag{29}
$$

Next, we evaluate the integrals in Eq. (29). The full result of this computation can be found in Appendix A. However, for the present discussion we focus only on the following terms:

$$
\rho(\mathbf{p}; \mathbf{p}'; t) = \rho(\mathbf{p}; \mathbf{p}'; 0) e^{-\mathrm{i}(E_{\mathbf{p}}^{\phi} - E_{\mathbf{p}'}^{\phi})t}
$$
$$
\times \left[1 - \frac{\mathrm{i}\alpha_2}{4} \left(\frac{1}{E_{\mathbf{p}}^{\phi}} - \frac{1}{E_{\mathbf{p}'}^{\phi}} \right) t \Delta_{zz}^{\mathrm{F}} \right.
$$
$$
\left. - \frac{\alpha_2^2}{32} \left(\frac{1}{E_{\mathbf{p}}^{\phi}} - \frac{1}{E_{\mathbf{p}'}^{\phi}} \right)^2 t^2 \Delta_{zz}^{\mathrm{F}} \Delta_{z'z'}^{\mathrm{F}} \right] + \mathcal{O}\left(\alpha_{1,2}^2\right).
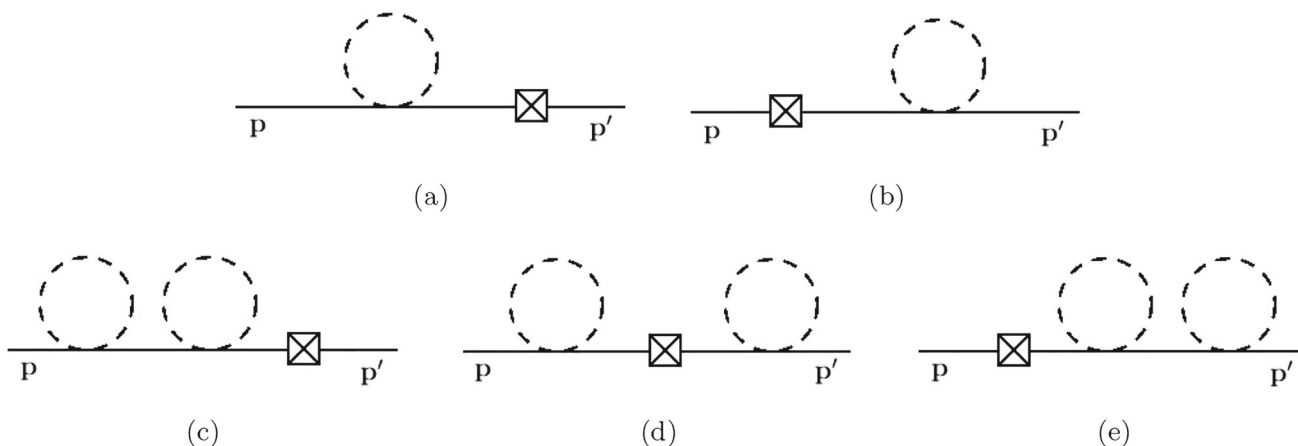\tag{30}
$$

Fig. 1 Diagrammatic representation of of the last two terms in the square brackets in Eq. (30); solid/dashed lines represent ϕ-/χ-propagators. Crossed boxes depict insertions of the initial density matrix

A diagrammatic depiction of the last two terms in the square brackets can be found in Fig. 1.

Following Ref. [50], we deal with the tadpoles in Eq. (30) by adding a counter term

$$\delta S_{\text{int}}[\phi, \chi] := \frac{\alpha_2}{4} \int_x \Delta_{xx}^{F(T=0)} \phi^2 \tag{31}$$

to the interaction action in Eq. (12), where $(T = 0)$ indicates the temperature-independent part of the χ-propagator. The thermal part

$$\Delta_{xx}^{F(T \neq 0)} = \int_k 2\pi f(|k^0|)\delta(k^2 + m^2)$$

$$= \frac{T^2}{2\pi^2} \int_{m/T}^{\infty} d\xi \frac{\sqrt{\xi^2 - (\frac{m}{T})^2}}{e^\xi - 1} \tag{32}$$

is by default finite in the ultraviolet. Using this, and identifying the terms in the square brackets of Eq. (30) as the expansion of an exponential function, we find

$$\rho(\mathbf{p}; \mathbf{p}'; t) = \rho(\mathbf{p}; \mathbf{p}'; 0) \exp$$

$$\times \left\{ -i \left[E_{\mathbf{p}}^\phi - E_{\mathbf{p}'}^\phi + \frac{\alpha_2}{4} \left(\frac{1}{E_{\mathbf{p}}^\phi} - \frac{1}{E_{\mathbf{p}'}^\phi} \right) \Delta_{zz}^{F(T \neq 0)} \right] t \right\}$$

$$+ \mathcal{O}\left(\alpha_{1,2}^2 \right). \tag{33}$$

Now we recall that we performed all computations with the rescaled mass M as given in Eq. (14). However, cp. with Ref. [50], experiments are actually sensitive to the absolute mass $\tilde{M}$. Rewriting Eq. (33), we obtain

$$\rho(\mathbf{p}; \mathbf{p}'; t) = \rho(\mathbf{p}; \mathbf{p}'; 0) \exp \left\{ -i \left[\tilde{E}_{\mathbf{p}}^\phi - \tilde{E}_{\mathbf{p}'}^\phi \right.\right.$$

$$\left. + \tilde{M}^2 \frac{A_2}{2M_{Pl}^2} \left(\langle X \rangle^2 + \Delta_{zz}^{F(T \neq 0)} \right) \right.$$

$$\times \left. \left(\frac{1}{\tilde{E}_{\mathbf{p}}^\phi} - \frac{1}{\tilde{E}_{\mathbf{p}'}^\phi} \right) \right] t \right\} + \mathcal{O}\left(\alpha_{1,2}^2 \right), \tag{34}$$

where $\tilde{E}_{\mathbf{p}}^\phi = \sqrt{\mathbf{p}^2 + \tilde{M}^2}$, we replaced α_2 by Eq. (15), and neglected the term $\sim \mathcal{O}(A_2^2 \tilde{M}^2 \langle X \rangle^2 / M_{Pl}^4)$. What we found in Eq. (34) is a first order correction to the unitary evolution term, i.e. a phase shift $\Delta u \cdot t$ with a frequency shift Δu. Other effects like de-/recoherence and momentum diffusion first appear at second order, see Appendix 1, and are therefore expected to be subdominant.

4 Predicted constraints

Atom interferometry experiments have successfully been used to constrain a variety of screened scalar field models [35,36,38,39,41,42,44]. As was also done in Ref. [50], we now estimate whether the frequency shift found in Eq. (34) could potentially be observed in an atom interferometer. Since such experiments use low-energy atoms, we make a non-relativistic approximation $\tilde{M}^2 \gg \mathbf{p}^2$, such that

$$\frac{1}{\tilde{E}_{\mathbf{p}}^\phi} \approx \frac{1}{\tilde{M}} \left(1 - \frac{\mathbf{p}^2}{2\tilde{M}^2} \right), \quad \frac{1}{\tilde{E}_{\mathbf{p}}^\phi} - \frac{1}{\tilde{E}_{\mathbf{p}'}^\phi} \approx \frac{v^2}{2\tilde{M}} \tag{35}$$

with $v := \frac{\|\mathbf{p}\| - \|\mathbf{p}'\|}{\tilde{M}}$ being the speed difference between the two atomic states. Substituting this into Eq. (34), gives for the frequency shift:

$$\Delta u := \tilde{M} \frac{A_2}{4M_{Pl}^2} \left[\langle X \rangle^2 + \Delta_{zz}^{F(T \neq 0)} \right] v^2. \tag{36}$$

For the estimation we choose commonly used values for the parameters of the experiment: a vacuum chamber with radius $L = 10$ cm [35,38], and a Rubidium-87 atom with a mass of $\tilde{M} = 87 \, m_u$ [44], where m_u is the atomic mass unit, as the
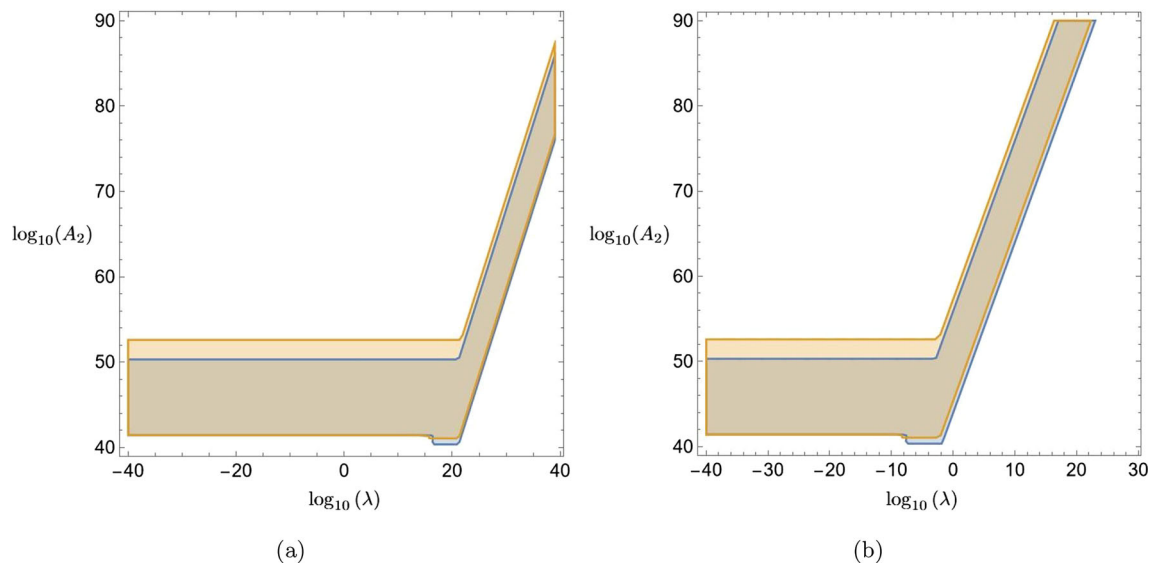
Fig. 2 Exclusion plots for the environment dependent dilaton (λ, A_2)-parameter space resulting from differences in frequency shifts $u(P_1, T_2; P_1, T_1)$ (blue) and $u(P_1, T_4; P_1, T_1)$ (orange); **a** $V_0 = 1\,\mathrm{eV}^4$, **b** $V_0 = 1\,(\mathrm{MeV})^4$

probe object. For the speed difference between the atomic states we use $v = 50$ mm s^{-1} [108]. In addition, from Refs. [108,109] we infer that in modern atom interferometry experiments frequency shifts as small as $\Delta u_{\min} \approx 10^{-8}$ Hz can be measured. For the dilaton's vev we follow the ansatz made in Ref. [50] and assume that the experiment takes place in a sufficiently small part in the center of the vacuum chamber, such that we can assume $\langle X \rangle$ to be approximately spatially constant. In addition, we only consider parts of the parameter space for which the Compton wavelength $\lambda_C = 1/m$ of the dilaton fulfils $\lambda_C \leq L$, such that the field is able to take on its proper vev and not an intermediate value. In order to also consider cases for which $\lambda_C > L$, we would need a sufficiently good model for the evolution of the field profile from within the vacuum chamber walls to the center of the chamber, as was developed for the chameleon, for example, in Ref. [39]. However, the sophisticated numerical studies required for this are beyond the scope of the present article.

A frequency shift is only a useful observable if we can compare it to another measurement without any frequency shift or at least with a frequency shifted by a different magnitude. Since the expression in Eq. (36) depends on some parameters that can easily be varied, two measurements with different predicted frequency shifts can be compared. If the resulting predicted difference in frequency shifts cannot be observed, this puts constraints on the dilaton parameter space. The parameters that we choose to vary are the temperature T of the vacuum chamber walls, which affects the thermal part of the χ-propagators, and the pressure P, which, if we assume that the residual gas inside the vacuum chamber has thermalized with the walls, determines the value of ρ^{ext} due

to $\rho^{\mathrm{ext}} = P m_{\mathrm{mol}}/(T R_{\mathrm{gas}})$ with m_{mol} being the molar mass of the residual gas and R_{gas} the universal gas constant, and consequently leads to different values of $\langle X \rangle$ and m. For the temperature, we consider four different values: $T_1 = 0.5 \times 10^{-3}$ K, $T_2 = 100$ K, $T_3 = 300$ K, and $T_4 = 500$ K. Ref. [44] reports a residual H$_2$ ($m_{\mathrm{mol}}(\mathrm{H}_2) = 2.016$ g/mol [110]) gas pressure of $P_2 = 9.6 \times 10^{-10}$ mbar for their experiment. However, as most extreme values, vacua with $P_1 \approx 10^{-17}$ mbar [111] can be reached, and atom interferometry experiments have been performed in warm vapors of rubidium ($m_{\mathrm{mol}}(\mathrm{Rb}) = 85.468$ g/mol [112]) atoms with pressures as high as $P_3 \approx 10^{-2}$ mbar [113].

We select two pairs of pressure and temperature, and compare the resulting difference in frequency shifts, which can only be observed if

$$|\Delta u(P_a, T_b) - \Delta u(P_c, T_d)| =: u(P_a, T_b; P_c, T_d) \geq \Delta u_{\min} \tag{37}$$

is fulfilled. Furthermore, our previous assumptions require us to demand $\lambda \langle X \rangle / M_{Pl} \ll 1$ and $\sqrt{A_2} \langle X \rangle / M_{Pl} \ll 1$. Using these restrictions, and choosing values for V_0, we plot the parts of the (λ, A_2)-space for which Eq. (37) is fulfilled. The resulting plots for a few selected examples can be found in Figs. 2, and 4. In case of an experimental null result, the shaded areas in these figures exclude the respective parts of the environment dependent dilaton parameter space.

In Fig. 2 we present cases for which the lowest possible pressure P_1 is used, but the temperature is varied. For Fig. 2a we select $V_0 = 1\,\mathrm{eV}^4$, and consider $u(P_1, T_2; P_1, T_1)$ (blue plot) and $u(P_1, T_4; P_1, T_1)$ (orange plot), while for Fig. 2b we use $V_0 = 1\,(\mathrm{MeV})^4$, and keep everything else the same. Looking at these figures, we observe that in case
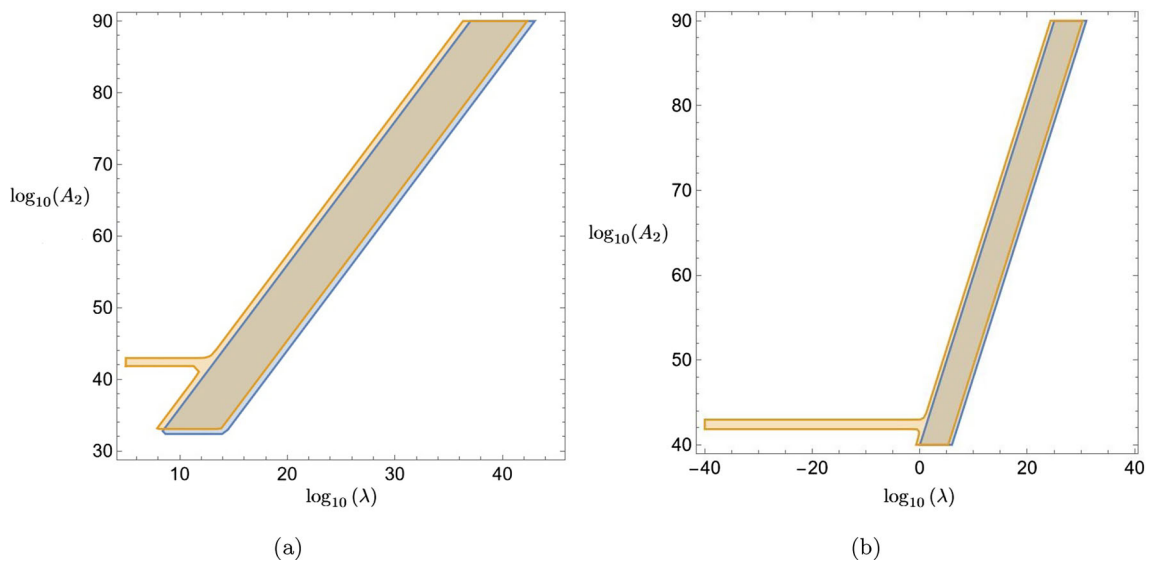
Fig. 3 Exclusion plots for the environment dependent dilaton (λ, A_2)-parameter space resulting from differences in frequency shifts $u(P_2, T_2; P_2, T_1)$ (blue) and $u(P_2, T_4; P_2, T_1)$ (orange); **a** $V_0 = 1\,(\text{keV})^4$, **b** $V_0 = 1\,(\text{MeV})^4$

of a null result, large parts of the dilaton parameter space could be excluded. Comparing frequency shifts with larger temperature differences, i.e. (T_4, T_1), extends the exclusion area. However, considering the lower temperature difference (T_2, T_1) adds comparatively small areas to the exclusion plots, which cannot be constrained with only (T_4, T_1). For the $V_0 = 1\,\text{eV}^4$ case, the horizontal exclusion area, which is more than 10 orders of magnitude in A_2 wide, stretches beyond $\lambda = 10^{20}$, while for $V_0 = 1\,(\text{MeV})^4$ it does not even reach $\lambda \approx 1$.

In Fig. 3 we consider P_2 and again vary the temperature, such that blue plots represent $u(P_2, T_2; P_2, T_1)$ and orange ones $u(P_2, T_4; P_2, T_1)$. Figure 3a depicts the case $V_0 = 1\,(\text{keV})^4$ and (b) $V_0 = 1\,(\text{MeV})^4$. Interestingly, the main difference between blue and orange shaded areas is that each orange one has a narrow (in A_2) horizontal section that cannot be found for the blue ones. Similarly to Fig. 2, going to higher values of V_0 lowers the values of λ that can be excluded by this section. However, here, the horizontal stripe is much shorter in Fig. 3a than in b.

Finally, in Fig. 4 we again consider the pressure P_2, but compare frequency shifts for the highest temperatures T_3 and T_4, i.e. we look at $u(P_2, T_4; P_2, T_3)$. The blue plot depicts the case $V_0 = 1\,\text{eV}^4$ and the orange one $V_0 = 1\,(\text{MeV})^4$. Both exclusion areas appear to be similar but shifted by more than 10 orders of magnitude on the λ-axis.

We do not find any exclusion areas for the highest pressure P_3 in combination with the other parameter values we chose. This can be explained by the rather large ρ^{ext} that results from the high pressure and temperatures in the considered warm rubidium vapors. A too dense environment suppresses the dilaton field, affecting the non-thermal part in Eq. (36), and
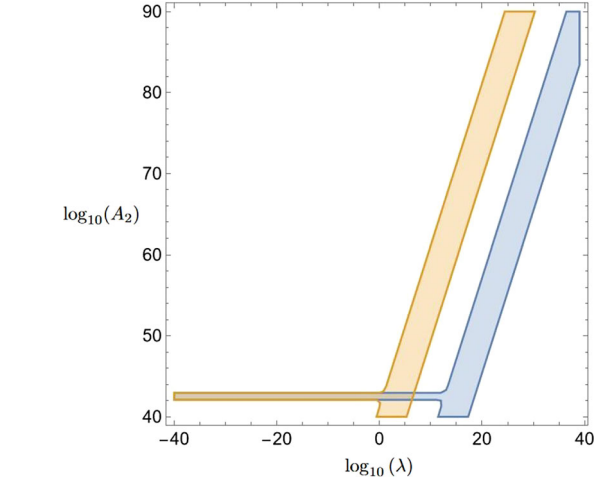

Fig. 4 Exclusion plots for the environment dependent dilaton (λ, A_2)-parameter space resulting from difference in frequency shifts $u(P_2, T_4; P_2, T_3)$; the blue plot represents $V_0 = 1\,\text{eV}^4$ and the orange plot $V_0 = 1\,(\text{MeV})^4$

increases its mass, which decreases the thermal part, such that the frequency shift predicted becomes too small to be observable.

5 Conclusions

Screened scalar fields are frequently used models in cosmology. Their screening mechanisms enable them to circumvent tight Solar-System constraints on their gravity-like fifth forces. However, it is possible to probe their parameter spaces in laboratory-based experiments like atom interferometry.

While other screened scalar field models like the chameleon or the symmetron are already experimentally well-studied, the parameter space of the environment dependent dilaton, motivated by string theory and screened by the Polyakov–Damour mechanism, is still largely unconstrained.

Recently, Ref. [59] presented a new path integral-based method for directly computing reduced density matrices of open quantum systems. In the present article, we applied this formalism to an open system modelled by the real, massive scalar field ϕ coupled to an environment comprising fluctuations χ of the dilaton field X. Following the study in Ref. [50], it was our intention to use ϕ as proxy for an atom in matter wave interferometry. For an atom, this was a rough, but, in this particular physical situation, suitable, first approximation since the dilaton only couples to the mass density. We improved the approximation by restricting the discussion to the single-particle momentum subspace, and neglecting all diagrams containing ϕ-loops since those would not appear at the considered perturbative order for complex composite objects like atoms. Using Ref. [59], we computed the single-particle density matrix element in a momentum basis at final time t under the assumption of an initial single atom at time 0. The resulting expression was presented in Appendix A. However, for the actual discussion, we focused only on the leading effect, which turned out to be a correction to the unitary evolution of ϕ. In an interferometry experiment, such a correction would be visible as a frequency shift if the measurement was compared to another one with a different or without any shifted frequency.

For realistic parameters of an atom interferometry experiment, we used this frequency shift in order to predict exclusion plots for the dilaton parameter space. While these predictions should be taken with care due to us approximating an atom by a scalar field, our investigation offers a glimpse at the full potential that open quantum dynamical effects have for studying and constraining physics beyond the standard models of particles and cosmology. Since the predicted exclusion plots look very promising, the present article, besides being the very first practical application of the formalism developed in Ref. [59], serves as a strong motivation for future studies with more realistic probe systems. Those will provide us with new, powerful tools for our search after screened scalar fields and even other candidate models for dark energy or dark matter.

Appendix A: Density matrix elements

Evaluating Eq. (29) gives us

$$\rho(\mathbf{p};\mathbf{p}';t) = \rho(\mathbf{p};\mathbf{p}';0)e^{-i(E_\mathbf{p}^\phi - E_{\mathbf{p}'}^\phi)t}\left\{1 - (2\pi)^3\delta^{(3)}(\mathbf{0})\left[\frac{\alpha_2^2}{8}\int_\mathbf{q}\frac{\sin^2(E_\mathbf{q}^\phi t)}{4(E_\mathbf{q}^\phi)^4}\Delta_{zz}^\mathrm{F}\Delta_{z'z'}^\mathrm{F}\right.\right.$$

$$+\frac{\alpha_1^2 M^2}{2}\int_{\mathbf{kq}}\frac{1}{2E_\mathbf{k}^\phi E_\mathbf{q}^\phi E_{\mathbf{q-k}}^\chi}\left(\frac{\sin^2\left(\frac{(E_\mathbf{k}^\phi + E_\mathbf{q}^\phi + E_{\mathbf{q-k}}^\chi)t}{2}\right)}{(E_\mathbf{k}^\phi + E_\mathbf{q}^\phi + E_{\mathbf{q-k}}^\chi)^2} + \sum_{a=\pm}\frac{\sin^2\left(\frac{(E_\mathbf{k}^\phi + E_\mathbf{q}^\phi + aE_{\mathbf{q-k}}^\chi)t}{2}\right)}{(E_\mathbf{k}^\phi + E_\mathbf{q}^\phi + aE_{\mathbf{q-k}}^\chi)^2}f(E_{\mathbf{q-k}}^\chi)\right)$$

$$+\frac{\alpha_2^2}{4}\int_{\mathbf{kql}}\frac{1}{2E_\mathbf{k}^\phi E_{\mathbf{k+q+l}}^\phi E_\mathbf{q}^\chi E_\mathbf{l}^\chi}\left(\sum_{a,b=\pm}\frac{\sin^2\left(\frac{(E_\mathbf{k}^\phi + E_{\mathbf{k+q+l}}^\phi + aE_\mathbf{q}^\chi + bE_\mathbf{l}^\chi)t}{2}\right)}{2(E_\mathbf{k}^\phi + E_{\mathbf{k+q+l}}^\phi + aE_\mathbf{q}^\chi + bE_\mathbf{l}^\chi)^2}f(E_\mathbf{q}^\chi)f(E_\mathbf{l}^\chi)\right.$$

$$+\frac{\sin^2\left(\frac{(E_\mathbf{k}^\phi + E_{\mathbf{k+q+l}}^\phi + E_\mathbf{q}^\chi + E_\mathbf{l}^\chi)t}{2}\right)}{2(E_\mathbf{k}^\phi + E_{\mathbf{k+q+l}}^\phi + E_\mathbf{q}^\chi + E_\mathbf{l}^\chi)^2} + \sum_{a=\pm}\frac{\sin^2\left(\frac{(E_\mathbf{k}^\phi + E_{\mathbf{k+q+l}}^\phi + E_\mathbf{q}^\chi + aE_\mathbf{l}^\chi)t}{2}\right)}{(E_\mathbf{k}^\phi + E_{\mathbf{k+q+l}}^\phi + E_\mathbf{q}^\chi + aE_\mathbf{l}^\chi)^2}f(E_\mathbf{l}^\chi)\left.\left.\right)\right]$$

$$-\frac{i\alpha_2}{4}\left(\frac{1}{E_\mathbf{p}^\phi} - \frac{1}{E_{\mathbf{p}'}^\phi}\right)t\Delta_{zz}^F - \frac{\alpha_2^2}{16}\left[\frac{1}{2}\left(\frac{1}{(E_\mathbf{p}^\phi)^2} - \frac{2}{E_\mathbf{p}^\phi E_{\mathbf{p}'}^\phi} + \frac{1}{(E_{\mathbf{p}'}^\phi)^2}\right)t^2\right.$$

$$+\left(\left(\frac{-i}{2(E_\mathbf{p}^\phi)^3}t + \frac{1 - e^{-2iE_\mathbf{p}^\phi t}}{4(E_\mathbf{p}^\phi)^4}\right) + (\mathbf{p}\longleftrightarrow\mathbf{p}')^*\right)\left.\right]\Delta_{zz}^\mathrm{F}\Delta_{z'z'}^\mathrm{F}$$

$$+i\alpha_1^2 M^2\int_\mathbf{q}\left[\frac{1}{8E_\mathbf{p}^\phi E_\mathbf{q}^\phi E_{\mathbf{p-q}}^\chi}\left(\sum_{a=\pm}\frac{\frac{i}{aE_\mathbf{p}^\phi + E_\mathbf{q}^\phi + E_{\mathbf{p-q}}^\chi}\left(1 - e^{-i(aE_\mathbf{p}^\phi + E_\mathbf{q}^\phi + E_{\mathbf{p-q}}^\chi)t}\right) + t}{aE_\mathbf{p}^\phi + E_\mathbf{q}^\phi + E_{\mathbf{p-q}}^\chi}\right.\right.$$

$$+\sum_{a,b=\pm}\frac{\frac{i}{aE_\mathbf{p}^\phi + E_\mathbf{q}^\phi + bE_{\mathbf{p-q}}^\chi}\left(1 - e^{-i(aE_\mathbf{p}^\phi + E_\mathbf{q}^\phi + bE_{\mathbf{p-q}}^\chi)t}\right) + t}{aE_\mathbf{p}^\phi + E_\mathbf{q}^\phi + bE_{\mathbf{p-q}}^\chi}f(E_{\mathbf{p-q}}^\chi)\left.\right) + (\mathbf{p}\longleftrightarrow\mathbf{p}')^*\right]$$

$$+i\frac{\alpha_2^2}{2}\int_{\mathbf{kq}}\left[\frac{1}{8E_\mathbf{p}^\phi E_{\mathbf{p-k-q}}^\phi E_\mathbf{k}^\chi E_\mathbf{q}^\chi}\left(\sum_{a=\pm}\frac{\frac{i}{aE_\mathbf{p}^\phi + E_{\mathbf{p-k-q}}^\phi + E_\mathbf{k}^\chi + E_\mathbf{q}^\chi}\left(1 - e^{-i(aE_\mathbf{p}^\phi + E_{\mathbf{p-k-q}}^\phi + E_\mathbf{k}^\chi + E_\mathbf{q}^\chi)t}\right) + t}{2(aE_\mathbf{p}^\phi + E_{\mathbf{p-k-q}}^\phi + E_\mathbf{k}^\chi + E_\mathbf{q}^\chi)}\right.\right.$$

$$+\sum_{a,b,c=\pm}\frac{\frac{i}{aE_\mathbf{p}^\phi + E_{\mathbf{p-k-q}}^\phi + bE_\mathbf{k}^\chi + cE_\mathbf{q}^\chi}\left(1 - e^{-i(aE_\mathbf{p}^\phi + E_{\mathbf{p-k-q}}^\phi + bE_\mathbf{k}^\chi + cE_\mathbf{q}^\chi)t}\right) + t}{2(aE_\mathbf{p}^\phi + E_{\mathbf{p-k-q}}^\phi + bE_\mathbf{k}^\chi + cE_\mathbf{q}^\chi)}f(E_\mathbf{k}^\chi)f(E_\mathbf{q}^\chi)$$

$$+\sum_{a,b=\pm}\frac{\frac{i}{aE_\mathbf{p}^\phi + E_{\mathbf{p-k-q}}^\phi + E_\mathbf{k}^\chi + bE_\mathbf{q}^\chi}\left(1 - e^{-i(aE_\mathbf{p}^\phi + E_{\mathbf{p-k-q}}^\phi + E_\mathbf{k}^\chi + bE_\mathbf{q}^\chi)t}\right) + t}{aE_\mathbf{p}^\phi + E_{\mathbf{p-k-q}}^\phi + E_\mathbf{k}^\chi + bE_\mathbf{q}^\chi}f(E_\mathbf{q}^\chi)\left.\right) - (\mathbf{p}\longleftrightarrow\mathbf{p}')^*\left.\right]\right\}$$

$$+\alpha_1^2 M^2\int_\mathbf{q}\rho(\mathbf{p-q};\mathbf{p}'-\mathbf{q};0)e^{-i(E_\mathbf{p}^\phi - E_{\mathbf{p}'}^\phi)t}\sum_{a=\pm}\left(e^{i(E_\mathbf{p}^\phi - E_{\mathbf{p-q}}^\phi - aE_\mathbf{q}^\chi)t} - 1\right)\left(e^{-i(E_{\mathbf{p}'}^\phi - E_{\mathbf{p}'-\mathbf{q}}^\phi - aE_\mathbf{q}^\chi)t} - 1\right)$$

$$\times\frac{af(aE_\mathbf{q}^\chi)}{8E_{\mathbf{p-q}}^\phi E_{\mathbf{p}'-\mathbf{q}}^\phi E_\mathbf{q}^\chi(E_\mathbf{p}^\phi - E_{\mathbf{p-q}}^\phi - aE_\mathbf{q}^\chi)(E_{\mathbf{p}'}^\phi - E_{\mathbf{p}'-\mathbf{q}}^\phi - aE_\mathbf{q}^\chi)} + \frac{\alpha_2^2}{2}\int_{\mathbf{kq}}\rho(\mathbf{p-k-q};\mathbf{p}'-\mathbf{k}-\mathbf{q};0)e^{-i(E_\mathbf{p}^\phi - E_{\mathbf{p}'}^\phi)t}$$

$$\times\sum_{a,b=\pm}\left(e^{i(E_\mathbf{p}^\phi - E_{\mathbf{p-k-q}}^\phi - aE_\mathbf{k}^\chi - bE_\mathbf{q}^\chi)t} - 1\right)\left(e^{-i(E_{\mathbf{p}'}^\phi - E_{\mathbf{p}'-\mathbf{k}-\mathbf{q}}^\phi - aE_\mathbf{k}^\chi - bE_\mathbf{q}^\chi)t} - 1\right)$$

$$\times\frac{abf(aE_\mathbf{k}^\chi)f(bE_\mathbf{q}^\chi)}{16E_{\mathbf{p-k-q}}^\phi E_{\mathbf{p}'-\mathbf{k}-\mathbf{q}}^\phi E_\mathbf{k}^\chi E_\mathbf{q}^\chi(E_\mathbf{p}^\phi - E_{\mathbf{p-k-q}}^\phi - aE_\mathbf{k}^\chi - bE_\mathbf{q}^\chi)(E_{\mathbf{p}'}^\phi - E_{\mathbf{p}'-\mathbf{k}-\mathbf{q}}^\phi - aE_\mathbf{k}^\chi - bE_\mathbf{q}^\chi)}. \tag{A1}$$

References

1. Y. Fujii, K. Maeda, *The Scalar-Tensor Theory of Gravitation. Cambridge Monographs on Mathematical Physics* (Cambridge University Press, Cambridge, 2003). https://doi.org/10.1017/CBO9780511535093

2. T. Clifton, P.G. Ferreira, A. Padilla, C. Skordis, Modified gravity and cosmology. Phys. Rep. **513**, 1 (2012). https://doi.org/10.1016/j.physrep.2012.01.001

3. A. Joyce, B. Jain, J. Khoury, M. Trodden, Beyond the cosmological standard model. Phys. Rep. **568**, 1 (2015). https://doi.org/10.1016/j.physrep.2014.12.002. arXiv:1407.0059

4. J.O. Dickey, P.L. Bender, J.E. Faller, X.X. Newhall, R.L. Ricklefs, J.G. Ries et al., Lunar laser ranging: a continuing legacy of the Apollo program. Science **265**, 482 (1994). https://doi.org/10.1126/science.265.5171.482

5. E. Adelberger, B. Heckel, A. Nelson, Tests of the gravitational inverse-square law. Annu. Rev. Nucl. Part. Sci. **53**, 77 (2003). https://doi.org/10.1146/annurev.nucl.53.041002.110503

6. D.J. Kapner, T.S. Cook, E.G. Adelberger, J.H. Gundlach, B.R. Heckel, C.D. Hoyle et al., Tests of the gravitational inverse-square law below the dark-energy length scale. Phys. Rev. Lett. **98**, 021101 (2007). https://doi.org/10.1103/PhysRevLett.98.021101

7. C. Burrage, J. Sakstein, Tests of Chameleon gravity. Living Rev. Relativ. **21**, 1 (2018). https://doi.org/10.1007/s41114-018-0011-x. arXiv:1709.09071

8. P. Brax, S. Casas, H. Desmond, B. Elder, Testing screened modified gravity. Universe **8**, 11 (2021). https://doi.org/10.3390/universe8010011. arXiv:2201.10817

9. J. Khoury, A. Weltman, Chameleon cosmology. Phys. Rev. D **69**, 044026 (2004). https://doi.org/10.1103/PhysRevD.69.044026. arXiv:astro-ph/0309411

10. J. Khoury, A. Weltman, Chameleon fields: awaiting surprises for tests of gravity in space. Phys. Rev. Lett. **93**, 171104 (2004). https://doi.org/10.1103/PhysRevLett.93.171104. arXiv:astro-ph/0309300

11. H. Dehnen, H. Frommert, F. Ghaboussi, Higgs field and a new scalar–tensor theory of gravity. Int. J. Theor. Phys. **31**, 109 (1992). https://doi.org/10.1007/BF00674344

12. E. Gessner, A new scalar tensor theory for gravity and the flat rotation curves of spiral galaxies. Astrophys. Space Sci. **196**, 29 (1992). https://doi.org/10.1007/BF00645239

13. T. Damour, A.M. Polyakov, The string dilaton and a least coupling principle. Nucl. Phys. B **423**, 532 (1994). https://doi.org/10.1016/0550-3213(94)90143-0. arXiv:hep-th/9401069

14. M. Pietroni, Dark energy condensation. Phys. Rev. D **72**, 043535 (2005). https://doi.org/10.1103/PhysRevD.72.043535

15. K.A. Olive, M. Pospelov, Environmental dependence of masses and coupling constants. Phys. Rev. D **77**, 043524 (2008). https://doi.org/10.1103/PhysRevD.77.043524

16. P. Brax, C. van de Bruck, A.-C. Davis, D. Shaw, Dilaton and modified gravity. Phys. Rev. D **82**, 063519 (2010). https://doi.org/10.1103/PhysRevD.82.063519

17. K. Hinterbichler, J. Khoury, Symmetron fields: screening long-range forces through local symmetry restoration. Phys. Rev. Lett. **104**, 231301 (2010). https://doi.org/10.1103/PhysRevLett.104.231301. arXiv:1001.4525

18. K. Hinterbichler, J. Khoury, A. Levy, A. Matas, Symmetron cosmology. Phys. Rev. D **84**, 103521 (2011). https://doi.org/10.1103/PhysRevD.84.103521. arXiv:1107.2112

19. C. Burrage, E.J. Copeland, P. Millington, Radial acceleration relation from symmetron fifth forces. Phys. Rev. D **95**, 064050 (2017). https://doi.org/10.1103/PhysRevD.95.064050. arXiv:1610.07529

20. C.A.J. O'Hare, C. Burrage, Stellar kinematics from the symmetron fifth force in the Milky Way disk. Phys. Rev. D **98**, 064019 (2018). https://doi.org/10.1103/PhysRevD.98.064019. arXiv:1805.05226

21. C. Burrage, E.J. Copeland, C. Käding, P. Millington, Symmetron scalar fields: modified gravity, dark matter, or both? Phys. Rev. D **99**, 043539 (2019). https://doi.org/10.1103/PhysRevD.99.043539. arXiv:1811.12301

22. C. Käding, Lensing with generalized symmetrons. Astron. **2**, 128 (2023). https://doi.org/10.3390/astronomy2020009. arXiv:2304.05875

23. M. Gasperini, F. Piazza, G. Veneziano, Quintessence as a runaway dilaton. Phys. Rev. D **65**, 023508 (2002). https://doi.org/10.1103/PhysRevD.65.023508. arXiv:gr-qc/0108016

24. T. Damour, F. Piazza, G. Veneziano, Violations of the equivalence principle in a dilaton runaway scenario. Phys. Rev. D **66**, 046007 (2002). https://doi.org/10.1103/PhysRevD.66.046007. arXiv:hep-th/0205111

25. T. Damour, F. Piazza, G. Veneziano, Runaway dilaton and equivalence principle violations. Phys. Rev. Lett. **89**, 081601 (2002). https://doi.org/10.1103/PhysRevLett.89.081601. arXiv:gr-qc/0204094

26. P. Brax, C. van de Bruck, A.-C. Davis, D. Shaw, The dilaton and modified gravity. Phys. Rev. D **82**, 063519 (2010). https://doi.org/10.1103/PhysRevD.82.063519. arXiv:1005.3735

27. P. Brax, C. van de Bruck, A.-C. Davis, B. Li, D.J. Shaw, Nonlinear structure formation with the environmentally dependent dilaton. Phys. Rev. D **83**, 104026 (2011). https://doi.org/10.1103/PhysRevD.83.104026. arXiv:1102.3692

28. P. Brax, H. Fischer, C. Käding, M. Pitschmann, The environment dependent dilaton in the laboratory and the solar system. Eur. Phys. J. C **82**, 934 (2022). https://doi.org/10.1140/epjc/s10052-022-10905-w. arXiv:2203.12512

29. G.R. Dvali, G. Gabadadze, M. Porrati, 4-D gravity on a brane in 5-D Minkowski space. Phys. Lett. B **485**, 208 (2000). https://doi.org/10.1016/S0370-2693(00)00669-9. arXiv:hep-th/0005016

30. A. Nicolis, R. Rattazzi, E. Trincherini, The Galileon as a local modification of gravity. Phys. Rev. D **79**, 064036 (2009). https://doi.org/10.1103/PhysRevD.79.064036. arXiv:0811.2197

31. A. Ali, R. Gannouji, M.W. Hossain, M. Sami, Light mass galileons: cosmological dynamics, mass screening and observational constraints. Phys. Lett. B **718**, 5 (2012). https://doi.org/10.1016/j.physletb.2012.10.009. arXiv:1207.3959

32. C. Burrage, J. Sakstein, A compendium of Chameleon constraints. JCAP **11**, 045 (2016). https://doi.org/10.1088/1475-7516/2016/11/045. arXiv:1609.01192

33. Y.N. Pokotilovski, Strongly coupled chameleon fields: possible test with a neutron Lloyd's mirror interferometer. Phys. Lett. B **719**, 341 (2013). https://doi.org/10.1016/j.physletb.2013.01.022. arXiv:1203.5017

34. Y.N. Pokotilovski, Potential of the neutron Lloyd's mirror interferometer for the search for new interactions. J. Exp. Theor. Phys. **116**, 609 (2013). https://doi.org/10.1134/S106377611309001X. arXiv:1311.4679

35. C. Burrage, E.J. Copeland, E.A. Hinds, Probing dark energy with atom interferometry. JCAP **03**, 042 (2015). https://doi.org/10.1088/1475-7516/2015/03/042. arXiv:1408.1409

36. P. Hamilton, M. Jaffe, P. Haslinger, Q. Simmons, H. Müller, J. Khoury, Atom-interferometry constraints on dark energy. Science **349**, 849 (2015). https://doi.org/10.1126/science.aaa8883. arXiv:1502.03888

37. H. Lemmel, P. Brax, A.N. Ivanov, T. Jenke, G. Pignol, M. Pitschmann et al., Neutron interferometry constrains dark energy chameleon fields. Phys. Lett. B **743**, 310 (2015). https://doi.org/10.1016/j.physletb.2015.02.063. arXiv:1502.06023

38. C. Burrage, E.J. Copeland, Using atom interferometry to detect dark energy. Contemp. Phys. **57**, 164 (2016). https://doi.org/10.1080/00107514.2015.1060058. arXiv:1507.07493

39. B. Elder, J. Khoury, P. Haslinger, M. Jaffe, H. Müller, P. Hamilton, Chameleon dark energy and atom interferometry. Phys. Rev. D **94**, 044051 (2016). https://doi.org/10.1103/PhysRevD.94.044051. arXiv:1603.06587

40. A.N. Ivanov, G. Cronenberg, R. Höllwieser, M. Pitschmann, T. Jenke, M. Wellenzohn et al., Exact solution for chameleon field, self-coupled through the Ratra-Peebles potential with $n = 1$ and confined between two parallel plates. Phys. Rev. D **94**, 085005 (2016). https://doi.org/10.1103/PhysRevD.94.085005. arXiv:1606.06867

41. C. Burrage, A. Kuribayashi-Coleman, J. Stevenson, B. Thrussell, Constraining symmetron fields with atom interferometry. JCAP **12**, 041 (2016). https://doi.org/10.1088/1475-7516/2016/12/041. arXiv:1609.09275

42. M. Jaffe, P. Haslinger, V. Xu, P. Hamilton, A. Upadhye, B. Elder et al., Testing sub-gravitational forces on atoms from a miniature, in-vacuum source mass. Nature Phys. **13**, 938 (2017). https://doi.org/10.1038/nphys4189. arXiv:1612.05171

43. P. Brax, M. Pitschmann, Exact solutions to nonlinear symmetron theory: one- and two-mirror systems. Phys. Rev. D **97**, 064015 (2018). https://doi.org/10.1103/PhysRevD.97.064015. arXiv:1712.09852

44. D.O. Sabulsky, I. Dutta, E.A. Hinds, B. Elder, C. Burrage, E.J. Copeland, Experiment to detect dark energy forces using atom interferometry. Phys. Rev. Lett. **123**, 061102 (2019). https://doi.org/10.1103/PhysRevLett.123.061102. arXiv:1812.08244

45. P. Brax, C. Burrage, A.-C. Davis, Laboratory constraints. Int. J. Mod. Phys. D **27**, 1848009 (2018). https://doi.org/10.1142/S0218271818480097

46. G. Cronenberg, P. Brax, H. Filter, P. Geltenbort, T. Jenke, G. Pignol et al., Acoustic Rabi oscillations between gravitational quantum states and impact on symmetron dark energy. Nat. Phys. **14**, 1022 (2018). https://doi.org/10.1038/s41567-018-0205-x. arXiv:1902.08775

47. D. Hartley, C. Käding, R. Howl, I. Fuentes, Quantum-enhanced screened dark energy detection. arXiv:1909.02272

48. M. Pitschmann, Exact solutions to nonlinear symmetron theory: one- and two-mirror systems II. Phys. Rev. D **103**, 084013 (2021). https://doi.org/10.1103/PhysRevD.103.084013. arXiv:2012.12752

49. P. Brax, S. Fichet, Quantum chameleons. Phys. Rev. D **99**, 104049 (2019). https://doi.org/10.1103/PhysRevD.99.104049. arXiv:1809.10166

50. C. Burrage, C. Käding, P. Millington, J. Minář, Open quantum dynamics induced by light scalar fields. Phys. Rev. D **100**, 076003 (2019). https://doi.org/10.1103/PhysRevD.100.076003. arXiv:1812.08760

51. C. Burrage, C. Käding, P. Millington, J. Minář, Influence functionals, decoherence and conformally coupled scalars. J. Phys. Conf. Ser. **1275**, 012041 (2019). https://doi.org/10.1088/1742-6596/1275/1/012041. arXiv:1902.09607

52. C. Käding, Astro- and quantum physical tests of screened scalar fields, Ph.D. thesis, University of Nottingham, Nottingham NG7 2RD, UK, 10, 2019. arXiv:1910.05738

53. D. Hartley, C. Käding, R. Howl, I. Fuentes, Quantum simulation of dark energy candidates. Phys. Rev. D **99**, 105002 (2019). https://doi.org/10.1103/PhysRevD.99.105002. arXiv:1811.06927

54. H.-P. Breuer, F. Petruccione, *The Theory of Open Quantum Systems* (Oxford University Press, Oxford, 2002)

55. M. Schlosshauer, *Decoherence and the Quantum-To-Classical Transition* (Springer, Berlin, 2007)

56. J.S. Schwinger, Brownian motion of a quantum oscillator. J. Math. Phys. **2**, 407 (1961). https://doi.org/10.1063/1.1703727

57. L.V. Keldysh, Diagram technique for nonequilibrium processes. Zh. Eksp. Teor. Fiz. **47**, 1515 (1964)

58. R.P. Feynman, F.L. Vernon, The theory of a general quantum system interacting with a linear dissipative system. Ann. Phys. **24**, 118 (1963)

59. C. Käding, M. Pitschmann, New method for directly computing reduced density matrices. Phys. Rev. D **107**, 016005 (2023). https://doi.org/10.1103/PhysRevD.107.016005. arXiv:2204.08829

60. C. Käding, M. Pitschmann, Density matrix formalism for interacting quantum fields. Universe **8**, 601 (2022). https://doi.org/10.3390/universe8110601. arXiv:2210.06991

61. H. Carmichael, *An Open Systems Approach to Quantum Optics: Lectures Presented at the Université Libre de Bruxelles, October 28 to November 4, 1991* (Springer, Berlin, 1993)

62. C. Gardiner, P. Zoller, *Quantum Noise: A Handbook of Markovian and Non-Markovian Quantum Stochastic Methods with Applications to Quantum Optics, Springer Series in Synergetics* (Springer, Berlin, 2004)

63. D. Walls, G. Milburn, *Quantum Optics* (Springer, Berlin, 2008)

64. L. Aolita, F. de Melo, L. Davidovich, Open-system dynamics of entanglement: a key issues review. Rep. Prog. Phys. **78**, 042001 (2015). https://doi.org/10.1088/0034-4885/78/4/042001

65. J. Goold, M. Huber, A. Riera, L. del Rio, P. Skrzypczyk, The role of quantum information in thermodynamics—a topical review. J. Phys. A Math. Theor. (2016). https://doi.org/10.1088/1751-8113/49/14/143001

66. A. Werner, D. Jaschke, P. Silvi, M. Kliesch, T. Calarco, J. Eisert et al., Positive tensor network approach for simulating open quantum many-body systems. Phys. Rev. Lett. (2016). https://doi.org/10.1103/physrevlett.116.237201

67. J. Huber, P. Kirton, S. Rotter, P. Rabl, Emergence of PT-symmetry breaking in open quantum systems. SciPost Phys. (2020). https://doi.org/10.21468/scipostphys.9.4.052

68. E.A. Calzetta, B.-L. Hu, *Nonequilibrium Quantum Field Theory* (Cambridge University Press, Cambridge, 2008)

69. J.F. Koksma, T. Prokopec, M.G. Schmidt, Decoherence in an interacting quantum field theory: the vacuum case. Phys. Rev. D **81**, 065030 (2010). https://doi.org/10.1103/PhysRevD.81.065030

70. J.F. Koksma, T. Prokopec, M.G. Schmidt, Decoherence in an interacting quantum field theory: thermal case. Phys. Rev. D **83**, 085011 (2011). https://doi.org/10.1103/PhysRevD.83.085011

71. L.M. Sieberer, M. Buchhold, S. Diehl, Keldysh field theory for driven open quantum systems. Rep. Prog. Phys. **79**, 096001 (2016)

72. J. Marino, S. Diehl, Quantum dynamical field theory for nonequilibrium phase transitions in driven open systems. Phys. Rev. B **94**, 085150 (2016). https://doi.org/10.1103/PhysRevB.94.085150

73. A. Baidya, C. Jana, R. Loganayagam, A. Rudra, Renormalization in open quantum field theory. Part I. Scalar field theory. JHEP **11**, 204 (2017). https://doi.org/10.1007/JHEP11(2017)204. arXiv:1704.08335

74. S. Nagy, J. Polonyi, Renormalizing open quantum field theories. Universe **8**, 127 (2022). https://doi.org/10.3390/universe8020127. arXiv:2012.13811

75. C. Jana, Aspects of open quantum field theory. Ph.D. thesis, Tata Inst. (2021)

76. H.C. Fogedby, Field-theoretical approach to open quantum systems and the Lindblad equation. Phys. Rev. A **106**, 022205 (2022). https://doi.org/10.1103/PhysRevA.106.022205. arXiv:2202.05203

77. F. Lombardo, F.D. Mazzitelli, Coarse graining and decoherence in quantum field theory. Phys. Rev. D **53**, 2001 (1996). https://doi.org/10.1103/PhysRevD.53.2001

78. F.C. Lombardo, D.L. Nacir, Decoherence during inflation: the generation of classical inhomogeneities. Phys. Rev. D **72**, 063506 (2005). https://doi.org/10.1103/PhysRevD.72.063506

79. F.C. Lombardo, Influence functional approach to decoherence during inflation. Braz. J. Phys. **35**, 391 (2005). https://doi.org/10.1590/S0103-97332005000300005. arXiv:gr-qc/0412069

80. D. Boyanovsky, Effective field theory during inflation: reduced density matrix and its quantum master equation. Phys. Rev. D **92**, 023527 (2015). https://doi.org/10.1103/PhysRevD.92.023527. arXiv:1506.07395

81. D. Boyanovsky, Effective field theory during inflation. II. Stochastic dynamics and power spectrum suppression. Phys. Rev. D **93**, 043501 (2016). https://doi.org/10.1103/PhysRevD.93.043501. arXiv:1511.06649

82. D. Boyanovsky, Fermionic influence on inflationary fluctuations. Phys. Rev. D **93**, 083507 (2016). https://doi.org/10.1103/PhysRevD.93.083507. arXiv:1602.05609

83. D. Boyanovsky, Imprint of entanglement entropy in the power spectrum of inflationary fluctuations. Phys. Rev. D **98**, 023515 (2018). https://doi.org/10.1103/PhysRevD.98.023515. arXiv:1804.07967

84. C.P. Burgess, R. Holman, G. Tasinato, M. Williams, EFT beyond the horizon: stochastic inflation and how primordial quantum fluctuations go classical. J. High Energy Phys. **2015**, 90 (2015). https://doi.org/10.1007/JHEP03(2015)090

85. T.J. Hollowood, J.I. McDonald, Decoherence, discord, and the quantum master equation for cosmological perturbations. Phys. Rev. D **95**, 103521 (2017). https://doi.org/10.1103/PhysRevD.95.103521

86. T. Binder, K. Mukaida, B. Scheihing-Hitschfeld, X. Yao, Non-Abelian electric field correlator at NLO for dark matter relic abundance and quarkonium transport. JHEP **01**, 137 (2022). https://doi.org/10.1007/JHEP01(2022)137. arXiv:2107.03945

87. S. Brahma, A. Berera, J. Calderón-Figueroa, Quantum corrections to the primordial tensor spectrum: open EFTs and Markovian decoupling of UV modes. JHEP **08**, 225 (2022). https://doi.org/10.1007/JHEP08(2022)225. arXiv:2206.05797

88. S. Brahma, A. Berera, J. Calderón-Figueroa, Universal signature of quantum entanglement across cosmological distances. Class. Quantum Gravity **39**, 245002 (2022). https://doi.org/10.1088/1361-6382/aca066. arXiv:2107.06910

89. T. Colas, J. Grain, V. Vennin, Benchmarking the cosmological master equations. Eur. Phys. J. C **82**, 1085 (2022). https://doi.org/10.1140/epjc/s10052-022-11047-9. arXiv:2209.01929

90. H.W. Yu, J. Zhang, H.-W. Yu, J.-L. Zhang, Understanding Hawking radiation in the framework of open quantum systems. Phys. Rev. D **77**, 024031 (2008). https://doi.org/10.1103/PhysRevD.77.029904. arXiv:0806.3602

91. F.C. Lombardo, G.J. Turiaci, Dynamics of an acoustic black hole as an open quantum system. Phys. Rev. D **87**, 084028 (2013). https://doi.org/10.1103/PhysRevD.87.084028. arXiv:1208.0198

92. C. Jana, R. Loganayagam, M. Rangamani, Open quantum systems and Schwinger–Keldysh holograms. JHEP **07**, 242 (2020). https://doi.org/10.1007/JHEP07(2020)242. arXiv:2004.02888

93. K. Agarwal, N. Bao, Toy model for decoherence in the black hole information problem. Phys. Rev. D **102**, 086017 (2020). https://doi.org/10.1103/PhysRevD.102.086017

94. G. Kaplanek, C.P. Burgess, Qubits on the horizon: decoherence and thermalization near black holes. JHEP **01**, 098 (2021). https://doi.org/10.1007/JHEP01(2021)098. arXiv:2007.05984

95. C.P. Burgess, R. Holman, G. Kaplanek, Quantum hotspots: mean fields, open EFTs, nonlocality and decoherence near black holes. arXiv:2106.10804

96. G. Kaplanek, C.P. Burgess, R. Holman, Qubit heating near a hotspot. JHEP **08**, 132 (2021). https://doi.org/10.1007/JHEP08(2021)132. arXiv:2106.10803

97. N. Brambilla, M.A. Escobedo, J. Soto, A. Vairo, Quarkonium suppression in heavy-ion collisions: an open quantum system approach. Phys. Rev. D **96**, 034021 (2017). https://doi.org/10.1103/PhysRevD.96.034021. arXiv:1612.07248

98. N. Brambilla, M.A. Escobedo, J. Soto, A. Vairo, Heavy quarkonium suppression in a fireball. Phys. Rev. D **97**, 074009 (2018). https://doi.org/10.1103/PhysRevD.97.074009. arXiv:1711.04515

99. X. Yao, T. Mehen, Quarkonium in-medium transport equation derived from first principles. Phys. Rev. D **99**, 096028 (2019). https://doi.org/10.1103/PhysRevD.99.096028. arXiv:1811.07027

100. X. Yao, T. Mehen, Quarkonium semiclassical transport in quark-gluon plasma: factorization and quantum correction. JHEP **02**, 062 (2021). https://doi.org/10.1007/JHEP02(2021)062. arXiv:2009.02408

101. Y. Akamatsu, Quarkonium in quark–gluon plasma: open quantum system approaches re-examined. Prog. Part. Nucl. Phys. **123**, 103932 (2022). https://doi.org/10.1016/j.ppnp.2021.103932. arXiv:2009.10559

102. W.A. De Jong, M. Metcalf, J. Mulligan, M. Płoskoń, F. Ringer, X. Yao, Quantum simulation of open quantum systems in heavy-ion collisions. Phys. Rev. D **104**, 051501 (2021). https://doi.org/10.1103/PhysRevD.104.L051501. arXiv:2010.03571

103. X. Yao, Open quantum systems for quarkonia. Int. J. Mod. Phys. A **36**, 2130010 (2021). https://doi.org/10.1142/S0217751X21300106. arXiv:2102.01736

104. N. Brambilla, M.A. Escobedo, M. Strickland, A. Vairo, P. Vander-Griend, J.H. Weber, Bottomonium production in heavy-ion collisions using quantum trajectories: differential observables and momentum anisotropy. Phys. Rev. D **104**, 094049 (2021). https://doi.org/10.1103/PhysRevD.104.094049. arXiv:2107.06222

105. P.V. Griend, Bottomonium observables in an open quantum system using the quantum trajectories method. EPJ Web Conf. **258**, 05005 (2022). https://doi.org/10.1051/epjconf/202225805005. arXiv:2111.13520

106. X. Yao, Quarkonium suppression in the open quantum system approach, in *19th International Conference on Hadron Spectroscopy and Structure, 1, 2022*. arXiv:2201.07702

107. G.C. Wick, The evaluation of the collision matrix. Phys. Rev. **80**, 268 (1950). https://doi.org/10.1103/PhysRev.80.268

108. B. Barrett, G. Condon, L. Chichet, L. Antoni-Micollier, R. Arguel, M. Rabault et al., Testing the universality of free fall using correlated 39k–87rb atom interferometers. AVS Quantum Sci. **4**, 014401 (2022)

109. B. Estey, C. Yu, H. Müller, P.-C. Kuan, S.-Y. Lan, High-resolution atom interferometers with suppressed diffraction phases. Phys. Rev. Lett. **115**, 083002 (2015)

110. National Center for Biotechnology Information, PubChem compound summary for CID 783, hydrogen. (2023). https://pubchem.ncbi.nlm.nih.gov/compound/Hydrogen

111. G. Gabrielse, X. Fei, L.A. Orozco, R.L. Tjoelker, J. Haas, H. Kalinowsky et al., Thousandfold improvement in the measured antiproton mass. Phys. Rev. Lett. **65**, 1317 (1990). https://doi.org/10.1103/PhysRevLett.65.1317

112. National Center for Biotechnology Information, PubChem compound summary for CID 5357696, rubidium. (2023). https://pubchem.ncbi.nlm.nih.gov/compound/Rubidium. Accessed 26 May 2023

113. G.W. Biedermann, H.J. McGuinness, A.V. Rakholia, Y.-Y. Jau, D.R. Wheeler, J.D. Sterk et al., Atom interferometry in a warm vapor. Phys. Rev. Lett. **118**, 163601 (2017). https://doi.org/10.1103/PhysRevLett.118.163601